NO chemisorption dynamics on thick FePc and ttbu-FePc films

N. L. Tran, S. R. Bishop, T. J. Grassman, G. C. Poon, F. I. Bohrer, W. C. Trogler, and A. C. Kummel[a)]
Department of Chemistry and Biochemistry, University of California San Diego, La Jolla, California 92039-0358, USA

(Received 3 September 2008; accepted 15 January 2009; published online 6 May 2009)

The NO chemisorption dynamics on ordered multilayer iron phthalocyanine (FePc) and quasiamorphous multilayer tetra-*t*-butyl FePc (ttbu-FePc) films on a Au(111) substrate was investigated using the King and Wells reflection technique. The NO zero coverage or initial sticking probabilities (S_0) were measured as a function of sample temperature (T_s) and beam energy (E_i). The experimental results for both films show a monotonic decrease in S_0 with increasing T_s and E_i consistent with NO adsorption occurring via a multiple pathway precursor-mediated mechanism in which the adsorbate initially physisorbs to the FePc organics, diffuses, and chemisorbs to the Fe metal center. The saturation coverage is 3% for the multilayer FePc surface and only 2% for the multilayer ttbu-FePc surface consistent with NO chemisorption occurring only on the Fe metal, where NO chemisorbs to 100% of the surface Fe metal centers. The reduced saturation coverage in the ttbu-FePc film is attributed to fewer Fe metal centers in the less dense ttbu-FePc films. A comparison of NO sticking on a multilayer FePc/Au(111) film with NO sticking on a monolayer FePc/Au(111) film shows that S_0 is greater on the multilayer FePc film for all T_s and E_i, consistent with an increase in collision inelasticity for NO/multilayer FePc/Au(111). © *2009 American Institute of Physics*. [DOI: 10.1063/1.3085808]

I. INTRODUCTION

Metallophthalocyanines (MPcs) are a group of square planar, metal coordination complexes in which a metal atom is bound by four pyrrole nitrogens linked to aromatic rings. MPcs can form highly ordered films and are chemically and thermally resilient. Initially, most studies on MPcs either focused on their use as blue and green dyestuffs[1] or compared their properties to similar organometallics, such as porphyrins.[2,3] MPcs are an attractive candidate for use in chemical sensors because a simple change of the metal atom[4–6] or substitution to the aromatics changes the gas chemisorption properties.[7,8] There are numerous studies on gas-induced changes in the MPc electronic structure but few studies on gas chemisorption dynamics on MPcs.[2,9–11] While a few sensor studies have focused on the different interactions of weak and strong binding analytes to MPcs,[12–14] nearly all experimental studies on MPc sensors neglect the basic mechanisms by which analytes absorb onto and react with MPcs.[15,16]

Recently, the King and Wells reflection technique has been used to investigate NO chemisorption dynamics on a monolayer FePc film in ultrahigh vacuum (UHV).[17] The experimental results are consistent with NO adsorbing to the monolayer FePc via a multiple pathway precursor-mediated mechanism in which the adsorbate first physisorbs to the FePc organics, then diffuses and chemisorbs to the Fe metal center. These findings were supported by density functional theory (DFT) simulations showing NO chemisorbs to the Fe metal center and physisorbs to all other nonmetal sites.[18] The DFT calculations showed that the barrier to NO diffusion between MPc adsorption sites on each MPc molecule was small suggesting that, at 300 K, NO can diffuse from the physisorption sites to the deep chemisorption well on the Fe metal.

The aforementioned study on NO/MPc chemisorption dynamics reported the sticking probability of NO on ordered monolayer FePc films, but MPc-based gas sensors are fabricated with multilayer MPc films.[13,19,20] This manuscript reports the effect of varying the nature of FePc-FePc interactions by measuring the NO sticking probabilities (S_0) on ordered multilayer FePc and quasiamorphous multilayer ttbu-FePc films as a function of sample temperature (T_s) and incident beam energy (E_i). In addition, the effect of FePc-FePc interactions versus FePc-Au(111) substrate interactions on adsorbate reactivity is investigated by comparing S_0 on the multilayer films versus S_0 on the ordered monolayer FePc film.

II. MATERIALS AND METHODS

The UHV chamber and molecular beam apparatus used in this study have been described in detail elsewhere.[21–23] A single crystal Au(111) substrate (Monocrystals, Inc.) was cleaned and ordered by sputtering with 2 kV Ar^+ ions followed by annealing the surface to 775 K for 5 min. Auger electron spectroscopy (AES) verified that the Au surface was free of impurities and low energy electron diffraction (LEED) showed that the surface order consisted of the expected $\sqrt{3}\times 22$ hexagonally closed-pack reconstruction.[24,25]

The sample temperature was controlled by liquid nitrogen cooling and radiative heating from the back side of the

[a)]Electronic mail: akummel@ucsd.edu.

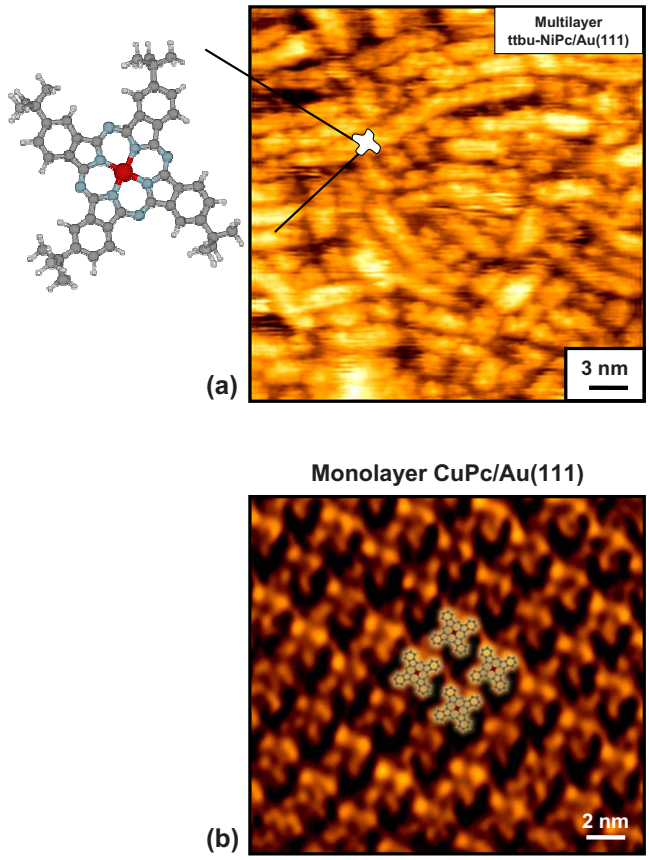

FIG. 1. (Color online) Filled-state STM image of (a) a multilayer tetra-*t*-butyl NiPc film on Au(111). Each organic ring is functionalized with tetra-*t*-butyl group and (b) an ordered monolayer CuPc on Au(111) superimposed with a schematic of four flat-lying MPc molecules. Both films have a flat surface. The multilayer ttbu-NiPc film contains short range order. Both STM images were obtained with −1.0 V sample bias and 0.5 nA tunneling current. Central atom=metal, azo- and pyrrole-atoms=nitrogen, gray =carbon, white=hydrogen.

sample with a thoriated iridium ribbon filament. T_s was varied from 100 to 300 K in 25 K increments. Supersonic NO molecular beams were directed at a normal angle to the FePc surface. NO was mixed with helium and neon to vary E_i; three translational beam energies were investigated: 0.4, 0.26, and 0.09 eV.[17]

The King and Wells beam reflectivity technique was employed to measure S_0.[26,27] The NO saturation coverage on both multilayer MPc films is calculated from the King and Wells sticking profiles, as described in Ref. 17, and found to occur on the order of 1–2 s.[17]

A. Ordered multilayer FePc

Fe(II)Pc powder was purchased from Sigma-Aldrich and purified by repeated degassing in the UHV chamber until the chamber pressure was below 10^{-7} Torr during deposition. A schematic of an FePc molecule can be found in Fig. 1(b). A multilayer FePc film was deposited onto the room temperature Au(111) substrate by maintaining a cell temperature of 615 K for 5 min (Createc low temperature effusion cell LTC-40-20-SH-M). The film was flash annealed to 375 K to desorb any residual contaminants remaining on the surface. Flash annealing the sample also facilitates in the formation of an ordered thick film that lies parallel to the substrate surface as demonstrated by various scanning tunneling microscopy (STM) and LEED studies.[28,29] The presence of a surface plane lying parallel to the substrate is important in this study since this exposed configuration allows the central Fe metal atom, the pyrrole and *meso*-nitrogens, and aromatics of the FePc molecule to freely interact with the incoming NO molecules. The AES spectrum of this surface consists of the expected carbon to nitrogen ratio of 4:1.[9] The Au peak is absent and consistent with the presence of a thick FePc film. The LEED pattern of the multilayer film taken at 15 eV results in the signature MPc/Au(111) diffraction pattern containing a superposition of three rotationally equivalent domains.[30] The Au diffraction pattern was not observed, also confirming the presence of a thick film.

B. Quasiamorphous multilayer ttbu-FePc

2(3), 9(10), 16(17), 23(24)-tetrakis-(*tert*-butyl)-phthalocyaninato iron (II), which will be referred to as tetra-*t*-butyl FePc (ttbu-FePc) in this study, was synthesized according to literature procedures.[31,32] For ttbu-FePc, each of the outer carbon rings has one *t*-butyl group randomly substituted for one of the hydrogens; therefore, the ttbu-FePc forms an amorphous bulk structure. A schematic of the substituted ttbu-FePc can be found in Fig. 1(a). 2.01 g of 1,2-dicyano-4-*tert*-butylbenzene (10.9 mmol) was dissolved in dry *N*,*N*-dimethylaminoethanol with 1.53 g of iron (II) sulfate heptahydrate (5.43 mmol) and 0.5 ml of 1,8-diazabicyclo[5.4.0]undec-7-ene. The solution was refluxed for 16 h. The product was cooled and precipitated in a 50:50 water/methanol solution, suction filtered, and washed several times with the 50:50 water/methanol solution. The resulting blue-black solid was further purified by Soxhlet filtration in acetone. The yield was 35%. The ttbu-FePc was initially purified by rough pumping at a sample temperature of 325 K. This was followed by a second purification process in which the sample was repeatedly degassed in the UHV chamber until the chamber pressure was below 10^{-7} Torr during deposition. The multilayer ttbu-FePc film was deposited onto the room temperature Au(111) substrate for 2 min at a cell temperature of 625 K and annealed at 575 K to desorb any residual contaminants from the film. Note that this annealing temperature is below the temperature at which ttbu-FePc sublimates. The AES spectrum of this surface results in the expected carbon to nitrogen ratio of 6:1 and an absence of the Au peak suggesting the presence of a thick film. No LEED pattern was observed for this surface, indicating that the ttbu-FePc film is at least partially amorphous. LEED is only sensitive to ordered domains in the *x*-*y* plane of about 90 nm so there may still be short-range order within the ttbu-FePc film. The higher energy residual pattern of the Au substrate was also not observed, consistent with the presence of a thick film.

The lack of order in the ttbu-FePc film agrees with Biswas *et al.* where they also found that tetra-*t*-butyl substituted MgPc formed a disordered thin film on Au(100) using photoelectron spectroscopy (PES).[33] In contrast to LEED and PES, the filled-state STM image (−1.0 V sample bias and

0.5 nA tunneling current) of a multilayer ttbu-NiPc film on Au(111), as shown in Fig. 1(a), clearly shows that substituted multilayer MPc films are not completely amorphous. Although the STM image provided is for a ttbu-NiPc/Au(111) film, whereas the sticking measurements are performed on a ttbu-FePc/Au(111) film, it has been shown that MPcs where the central metal consists of first row transition metals pack in an identical manner.[34] For MPc films on a Au(111) substrate, it has been shown that the lattice constants are similar for CuPc, NiPc, and FePc films.[35,36] This similarity permits the use of STM images for CuPc (see below) and ttbu-NiPc films in the following discussion of FePc and ttbu-FePc film structure and packing density. To minimize confusion, the STM images for CuPc/Au(111) and ttbu-NiPc/Au(111) will be referred to as the generic MPc and ttbu-MPc. Although the ttbu-MPc surface layer is missing the orientational and periodic long-range order that is observable by LEED, the STM image shows that it still has a nearly planar structure such that most of the metal centers, nitrogens, and aromatics are available for gas adsorption as in the ordered, multilayer MPc film.

A rough estimate of the areal density of flat-lying ttbu-MPc molecules can be extrapolated from the STM image in Fig. 1(a) by measuring the distance between the irregular rows of ttbu-MPc molecules. Numerous line scans on an 800×800 Å^2 ttbu-MPc/Au(111) film were measured to give an average ttbu-MPc row to row distance of 20.2 ± 3.7 Å. Using 20.2 ± 3.7 Å as the square planar lattice constant for the ttbu-MPc film, the maximum area occupied by a single ttbu-MPc molecule is estimated as 408 Å^2. Alternatively, a minimum areal density for ttbu-MPc is estimated by assuming an asymmetric unit cell made up of the ttbu-MPc/Au(111) row spacing and MPc/Au(111) lattice constant since the spacing within the ttbu-MPc row may be smaller than the spacing between the rows. The filled-state monolayer CuPc/Au(111) STM image in Fig. 1(b) (−1.0 V sample bias and 0.5 nA tunneling current) has a square lattice of 15.4 $\times$15.4 Å^2, in good agreement with Chizhov *et al.*[30] Using this lattice constant value with the ttbu-MPc/Au(111) row spacing, the estimated minimum areal density for a ttbu-MPc molecule is 311 Å^2. Therefore, surface ttbu-MPc molecules have an areal density between 24% and 42% lower than MPc molecules in the ordered monolayer or multilayer MPc films on Au(111).

III. RESULTS AND DISCUSSION

A. NO sticking on ordered multilayer FePc, multilayer ttbu-FePc, and monolayer FePc films

S_0 on the ordered multilayer FePc film versus T_s for all three NO beam energies are shown in Fig. 2(a). Note that NO sticking onto the Au(111) surface does not contribute to the S_0 values because NO does not stick to Au at these temperatures.[17,34] NO sticks to the multilayer film with $S_0=0.43\pm0.01$ at the lowest $E_i=0.09$ eV and $T_s=100$ K. Increasing E_i decreases S_0 to 0.38 ± 0.01 and 0.35 ± 0.01 for the 0.26 and 0.40 eV beams at 100 K, respectively. Increasing T_s linearly decreases the sticking probability such that $S_0=0.14\pm0.01$ at 300 K for the 0.09 eV beam. A similar

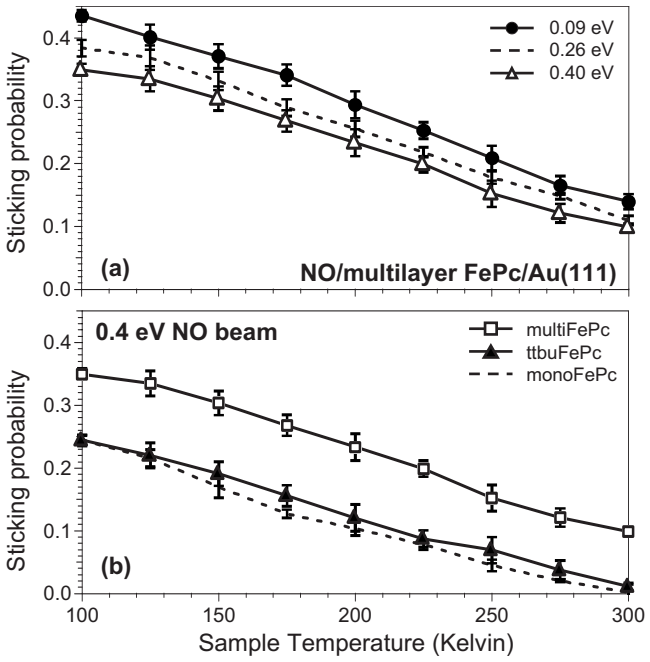

FIG. 2. Plot of NO sticking probabilities as a function of sample temperature at (a) varying NO beam energies (0.09 eV=filled circles, 0.26 eV=dashed line, and 0.40 eV=open triangles) for the multilayer FePc film and (b) 0.4 eV NO beam for the multilayer FePc (open squares), multilayer ttbu-FePc (filled triangles), and monolayer FePc (dashed line) films. All error bars shown are for the standard error of eight measurements at each temperature.

linear decrease in S_0 as a function of increasing T_s is also observed at higher beam energies. NO sticking even at 300 K is consistent with a final chemisorbed state since physisorbates are not stable on the surface at 300 K. A direct chemisorption model to explain NO adsorption onto the ordered multilayer FePc film can be excluded since direct chemisorption requires S_0 to be independent of T_s and sometimes E_i.[35–37] Instead, the strong dependence of S_0 on E_i and T_s observed in this study is consistent with NO precursor-mediated chemisorption onto the ordered multilayer FePc film. In the standard model of precursor-mediated chemisorption, NO traps onto the film prior to chemisorption; an increase in E_i or T_s decreases the trapping probability and an increase in T_s also increases the desorption probability of NO from the trapped state prior to chemisorption.[35,38,39]

To examine the effect of varying the nature of FePc-FePc interactions with FePc on Au(111) substrate interactions, a plot of S_0 of the 0.4 eV NO beam versus T_s onto an ordered multilayer FePc, quasiamorphous multilayer ttbu-FePc, and ordered monolayer FePc film is shown in Fig. 2(b). (The sticking measurements for the 0.4 eV NO beam onto the monolayer film were obtained in the previous King and Wells study.) S_0 is greater on the ordered multilayer FePc film (0.35 ± 0.01) than on both the multilayer ttbu-FePc (0.24 ± 0.03) and monolayer FePc films (0.24 ± 0.01) at 100 K. This trend is also observed at higher T_s, where S_0 for the ordered multilayer and quasiamorphous multilayer films are 0.099 ± 0.006 and 0.011 ± 0.008 at 300 K, respectively. S_0 is greater on the ordered multilayer FePc film than on the ttbu-FePc and monolayer FePc films at all T_s and E_i, whereas S_0 for the monolayer FePc and ttbu-FePc films are nearly

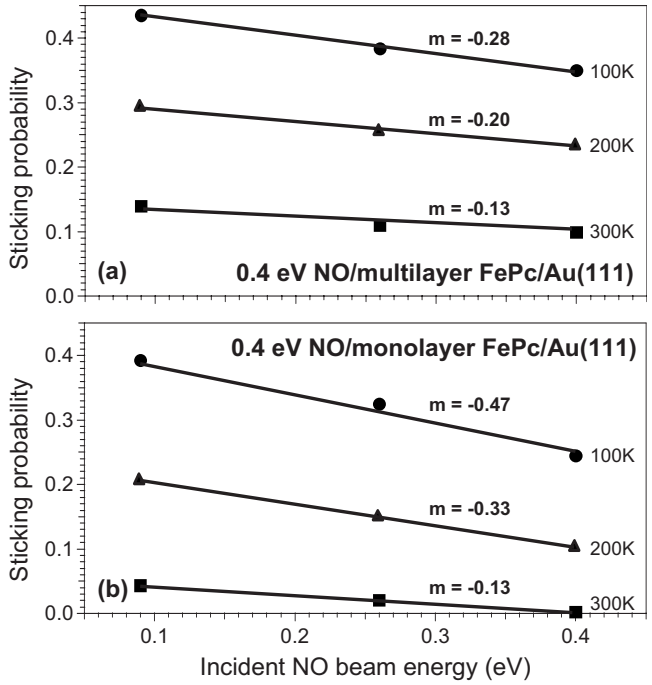

FIG. 3. Plot of NO sticking probability as a function of beam energy at 100, 200, and 300 K for the (a) ordered multilayer FePc and (b) ordered monolayer FePc films. All linear fits have a regression coefficient, R^2, greater than 0.95.

identical at all T_s and E_i. While the overall sticking of NO to the multilayer ttbu-FePc film and monolayer FePc films is less than that for the ordered multilayer FePc film, NO adsorption onto the ttbu-FePc and monolayer FePc films shows a similar trend, whereby increasing T_s linearly decreases S_0. The monotonic decrease in S_0 with increased T_s suggests that NO undergoes precursor-mediated chemisorption onto all three films.

For NO sticking onto the multilayer ttbu-FePc film, the lower S_0 at all T_s and E_i may be due to a more convoluted path to diffusion between the physisorption and chemisorption sites and due to a lower density of each type of adsorption site. The addition of *t*-butyl groups on the aromatics may create additional NO physisorption sites in a system that already possesses six distinct physisorption sites in the form of the aromatics and the *meso*- and pyrrole nitrogens.[18] However, the bonding of NO to the relatively nonreactive *t*-butyl carbons is likely to be weaker than that to the aromatic sites. Moreover, the nearly identical temperature dependence of S_0 for both the ordered thick FePc and quasiamorphous ttbu-FePc films is most consistent with the *t*-butyl group being inert to NO physisorption over the full temperature range studied. Therefore, the lower S_0 on the thick ttbu-FePc film is primarily attributed to fewer metal, aromatic, and nitrogen sites being exposed to the incoming beam due to its lower packing density.

For NO sticking onto the ordered monolayer FePc films, the lower S_0 is consistent with a greater NO trapping probability on the ordered multilayer FePc film due to enhanced inelastic collisions in the effectively lighter multilayer FePc/Au(111) film compared to the heavier monolayer FePc/Au(111) film. As shown in Figs. 3(a) and 3(b), plotting the NO sticking probability as a function of NO beam energy for both the ordered monolayer and ordered multilayer FePc films shows a linear dependence of S_0 on E_i. Linearly fitting S_0 as a function of E_i at 100 K for the multilayer FePc film/Au(111) gives a slope of −0.28. Increasing T_s to 200 and 300 K decreases the slope to −0.20 and −0.13. As shown in Fig. 3(b), the same fit for NO sticking onto the monolayer FePc film/Au(111) at 100 K results in a slope of −0.47 or 1.7 times greater than for the ordered multilayer FePc film. Increasing T_s to 200 K also results in a slope that is 1.7 times greater than for the ordered thick film until, at 300 K, the slopes are nearly identical. The equivalent slopes at 300 K suggest that at higher T_s, the NO trapping probability onto the ordered multilayer FePc and monolayer FePc films is no longer a crucial factor in NO adsorption onto these films. However, the differences in slopes at lower T_s are consistent with a higher density of soft phonon modes in the multilayer FePc film compared to the monolayer FePc film. By examining the effective mass difference between the ordered films, a qualitative comparison of the collision elasticity can be made. The effective mass of the Fe metal chemisorption site on the multilayer FePc/Au(111) can be calculated by adding the mass of the Fe metal center of the surface FePc and the Fe metal center of the FePc directly below the surface layer. The effective mass of the Fe metal chemisorption site on the monolayer FePc/Au(111) can be calculated similarly, whereby the layer directly below the surface Fe consists of a heavy Au substrate atom. This results in an effective mass of 101 amu for the Fe metal chemisorption site on the multilayer FePc/Au(111) film and 253 amu for the Fe metal chemisorption site on the monolayer FePc/Au(111). Therefore, the inferior mass matching between the NO molecule and the monolayer FePc/Au(111) film reduces the "heavier" film's ability to trap NO compared to the "lighter" ordered multilayer FePc/Au(111) film. In addition to playing a mechanical role in affecting NO adsorption onto the monolayer FePc film, the Au substrate may affect NO adsorption by perturbing the FePc electronic structure in the monolayer film compared to the multilayer FePc film. Although a previous computational study showed that the NO binding strength onto a single FePc molecule (monomer) and a vertical stack of three FePc molecules (trimer) are nearly identical, substrate effects were not included in the simulations.[18] A recent STM study investigated the electronic structure of a monolayer CoPc/Au(111) film and a trilayer CoPc/Au(111) film.[40] By analyzing the range in bias voltages (−2–+2 V) in which the CoPc molecules were observed, Takada and Tada showed that the electronic structure of the monolayer film was more delocalized than the trilayer film, suggesting that the Au substrate does perturb the phthalocyanine electronic structure.

Film roughness may also affect NO adsorption onto the three different films. To further investigate this, the effect of film roughness on gas adsorption was studied indirectly on MPc films deposited on SiO_2. On SiO_2, MPc adsorbs in an α-polymorph structure with metal centers exposed only at step edges. No effect of roughness was observed on the mobility in air consistent with roughness having little influence on the adsorption of O_2 and H_2O.[41] Therefore, it is expected

that roughness will have no effect on NO adsorption on MPc/Au(111) since the MPc lie flat on this surface and should be less influenced by roughness than MPc/SiO_2.

In sum, the greater S_0 at all T_s and E_i suggests that the ordered multilayer FePc film possesses a greater ability to trap NO onto the aromatics than both the quasiamorphous ttbu-FePc and monolayer FePc films. While S_0 for the ttbu-FePc and monolayer FePc films are nearly identical, the explanation for the attenuated sticking is not. The lower S_0 on the thick ttbu-FePc film is attributed to the exposure of fewer metal, aromatic, and nitrogen sites to the NO beam due to its lower packing density. However, this is not the case for the monolayer FePc film since the packing densities of the ordered multilayer FePc and monolayer FePc films are identical. Instead, the lower S_0 on the monolayer FePc film is attributed to a reduction in the degree of inelastic collisions due to the heavy Au substrate atoms. In addition, the Au substrate may also play a role in perturbing the electronic structure of the monolayer FePc film to affect NO trapping.

B. NO saturation coverage on multilayer FePc, multilayer ttbu-FePc, and monolayer FePc films

Since the area of the FePc molecule occupied by the Fe metal center is small, NO saturation coverage should also be small. A previous study showed that the area occupied by the Fe metal center in the monolayer FePc films was roughly 3%.[17] The normalized NO saturation coverage on both multilayer FePc films can be derived by integrating the area of the sharp, downward spike in the NO/multilayer FePc sticking profiles and calculating the ratio of this integrated area with respect to the integrated area of the NO/Al(111) sticking profiles, since NO has a 1 ML saturation coverage on Al(111).[17,42] This technique is explained in detail in Ref. 17. The normalized NO saturation coverage on the ordered multilayer FePc film versus T_s is shown in Fig. 4(a) for all three E_i. NO saturation on the ordered multilayer FePc film for all three E_i is approximately 3% from 100 to 225 K. At temperatures above 225 K, the total saturation coverage gradually decreases. A saturation coverage of 3% is consistent with the NO chemisorption site on the multilayer FePc film being restricted to the Fe metal center where NO chemisorbs to 100% of the surface Fe metal centers. The organic component of the FePc molecule acts as precursor physisorption sites prior to NO diffusion to the metal. The high sticking probability ranging from 24% to 44% at 100 K for all three films and all three beam energies despite a 3% active surface suggests a steering effect or a mobile precursor. Since the sticking probability decreases with surface temperature, a mobile precursor is indicated where the NO molecules initially adsorb onto the organic ligands and migrate to the Fe metal center.[43] Published DFT simulations of the site specific binding of NO onto an FePc monomer showing a small barrier to diffusion from organic site to organic site (~0.1–0.2 eV) also support a mobile precursor since these barriers can be overcome at room temperature.[18]

The attenuation in saturation coverage at higher T_s may be due to NO approaching the desorption temperature from the ordered multilayer FePc film. However, the calculation

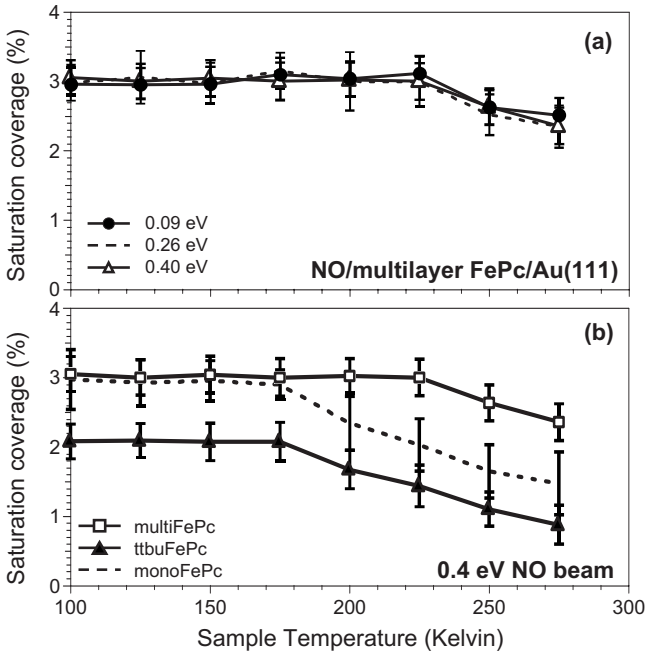

FIG. 4. Plot of NO saturation coverage as a function of sample temperature at (a) varying NO beam energies for a multilayer FePc film and (b) 0.4 eV NO beam for the multilayer FePc (open squares), multilayer ttbu-FePc (filled triangles), and monolayer FePc (dashed line) films. Note that NO saturation values of 3% and 2% are consistent with NO chemisorption on 100% of the surface Fe metal center sites for all three FePc films. The error bars shown are for the standard deviation of the error where eight measurements were performed at each temperature.

method used to determine the saturation coverage may also contribute to the decrease in saturation coverage beginning at 225 K. As T_s increases, S_0 decreases, making the calculation of the area in the spike less accurate since short wide spikes at higher T_s are not as well defined as the tall narrow spikes at lower T_s. These shallow and ill-defined spikes make determination of the cutoff point with which to integrate the spike difficult at high temperature.

For NO saturation on the quasiamorphous multilayer ttbu-FePc film, a smaller saturation coverage is expected since the ttbu-FePc film contains a lower surface molecular density than the ordered multilayer FePc film. As discussed above in Sec. III B, the multilayer ttbu-FePc film is approximately 24%–42% less dense than the multilayer FePc film. This suggests that the total area occupied by the metal centers in the ttbu-FePc film should also be 24%–42% less than in the ordered multilayer FePc film. Therefore, the area occupied by the Fe metal centers in the quasiamorphous film should be 2.27%–1.73%. In contrast, NO saturation on the monolayer FePc and multilayer FePc films should be identical since both films are highly ordered and contain the same areal density. As seen in Fig. 4(b), NO saturation coverage on the quasiamorphous ttbu-FePc film is ~2% from 100 to 175 K; this is less than the 3% observed for the ordered multilayer FePc film and essentially the midpoint of the predicted range for the less dense ttbu-FePc film. A saturation coverage of 2% is consistent with the NO chemisorption site on the multilayer ttbu-FePc film also being restricted to the Fe metal center where NO chemisorbs to 100% of the surface Fe metal centers. The organic component of the ttbu-

FePc molecule acts as precursor physisorption sites prior to NO diffusion to the metal. As expected, the NO saturation coverage on the monolayer FePc film from 100 to 175 K is 3% and identical to the saturation coverage on the multilayer FePc film.

While NO saturation coverage on the ordered multilayer FePc film gradually decreases beginning at 225 K, the coverage decrease in the multilayer ttbu-FePc and monolayer FePc films begins at a lower temperature, 175 K. There are two possible explanations. First, NO desorption from the multilayer ttbu-FePc film occurring at a lower temperature than the ordered multilayer FePc film would be consistent with the NO chemisorption well on the Fe metal center being more shallow on the multilayer ttbu-FePc film than on the multilayer FePc film. This hypothesis is consistent with a recent STM study, showing that the electronic structure of surface CoPc molecules is different on monolayer and trilayer CoPc films on Au(111).[40] However, Tran *et al.* showed that NO binding onto the Fe metal center of a single FePc molecule (monomer), a system with zero possibility for Fe-Fe metal interaction and an FePc triple stack (trimer), a system that maximizes the potential for metal-metal interaction, have nearly equivalent exothermicity.[18] The second explanation of lower temperature for attenuation in saturation coverage on the quasiamorphous ttbu-FePc and monolayer FePc films versus the ordered multilayer FePc film is the error inherent in the calculation method. For high S_0, the spike is prominent and well defined, whereas the spike for low S_0 is shallow and ill defined. An ill-defined spike makes determination of the cutoff point for spike integration and calculation of the saturation coverage difficult. Since S_0 is smaller at all sample temperatures for the quasiamorphous ttbu-FePc and the ordered monolayer FePc films, determining the saturation coverage for these films becomes problematic at lower sample temperatures compared to the ordered multilayer FePc film.

C. Precursor-mediated chemisorption model

For all NO beam energies studied, the S_0 observed at 100 K on the various FePc/Au(111) films are large ($0.24 < S_0 < 0.43$) even though the areas occupied by the Fe metal center in the ordered multilayer FePc and multilayer ttbu-FePc films are considerably smaller at 3% and 2%, respectively. This suggests that NO physisorbs to the aromatics and nitrogens on the FePc molecule prior to chemisorbing onto the Fe metal center. The strong linear dependence of S_0 on T_s for all three films and all E_i suggests that increasing the T_s decreases the number of available NO physisorption sites since the shallower physisorption sites are unable to promote NO chemisorption at higher surface temperatures. To quantify the distribution of physisorption sites on the various FePc films, the S_0 data for all three films were plotted in an Arrhenius form as discussed in detail in the previous study.[17] Analyzing the slope of the Arrhenius plot of S_0 and inverse T_s provides information on the difference between activation barriers for desorption versus chemisorption from the physisorption sites.

As shown in Fig. 5, the Arrhenius plot for the 0.4 eV NO/ttbu-FePc/Au(111) sticking data requires multiple linear fits to appropriately describe the curve. Note that the Arrhenius fits for NO/monolayer FePc/Au(111) were not shown since the monolayer results were nearly identical to the NO/ttbu-FePc/Au(111) results. The Arrhenius fits for the NO/monolayer FePc/Au(111) data have been previously reported.[17] Fitting the ttbu-FePc Arrhenius data to three separate lines results in three apparent barriers to chemisorption for NO adsorption onto the multilayer ttbu-FePc and monolayer FePc films ranging from very small barriers of 11 ± 2 meV (100–175 K) and 43 ± 2 meV (175–225 K) to larger barriers of 170 ± 79 meV (250–300 K). The various barriers to NO chemisorption from 100 to 300 K suggest that NO physisorption onto the multilayer ttbu-FePc/Au(111) and monolayer FePc/Au(111) films contains many distinct sites and pathways prior to chemisorption. All linear fits were chosen such that an optimal regression coefficient, R^2, was obtained. Note that the low temperature fit remaining linear from 100 to 175 K coincides with the saturation coverage remaining at its maximum of 2% from 100 to 175 K for NO adsorption on the multilayer ttbu-FePc and ordered monolayer FePc films. The ratio of the pre-exponential terms for the three temperature ranges were plotted and shown to vary: 7–10 from 100 to 175 K, 35–98 from 175 to 225 K, and greater than 7.75×10^5 from 250 to 300 K.

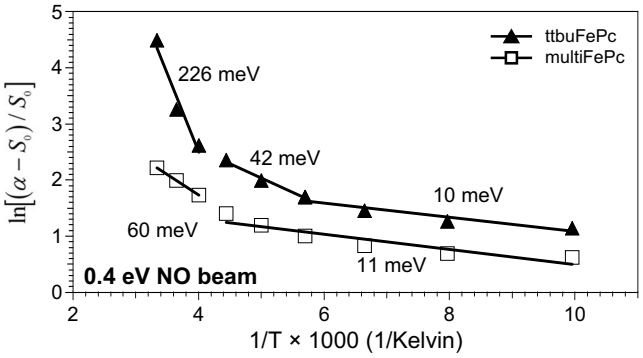

FIG. 5. Arrhenius plots for the 0.4 eV NO beam for the multilayer FePc (open squares) and multilayer ttbu-FePc (filled triangles) films. The monolayer FePc data were not shown as the results were nearly identical to the ttbu-FePc results.

For the NO/multilayer FePc/Au(111) sticking data, a bilinear fit sufficiently describes the Arrhenius plot. All linear fits were chosen such that an optimal regression coefficient, R^2, was obtained. In contrast to the NO/multilayer ttbu-FePc/Au(111) fit, the low temperature fit remained linear up to 225 K, consistent with the NO saturation coverage remaining at its maximum of 3% from 100 to 225 K. Similar to the monolayer FePc and multilayer ttbu-FePc films, the magnitudes of barriers to NO chemisorption on the ordered multilayer FePc film are also small (11 ± 1 meV from 100 to 225 K and 62 ± 5 meV from 250 to 300 K). In addition, the ratio of the pre-exponential terms for the two temperature ranges were plotted and shown to vary: 4.7–6.6 from 100 to 225 K and 71–129 from 250 to 300 K. The multiple barriers to chemisorption suggest that NO physisorption onto the multilayer FePc film also takes place at distinct sites and pathways as in the multilayer ttbu-FePc and monolayer FePc films.

IV. CONCLUSIONS

The King and Wells reflection technique was used to elucidate the chemisorption dynamics of NO on various FePc films. The results show that NO undergoes precursor-mediated chemisorption on all films studied: the ordered multilayer FePc film, the quasiamorphous multilayer ttbu-FePc film, and the ordered monolayer FePc film. The NO sticking probability is greatest on the multilayer FePc film and nearly identical between the multilayer ttbu-FePc and monolayer FePc films. The lower S_0 on the monolayer FePc film is ascribed to a lower density of soft phonon modes that may diminish the extent of inelastic collisions to decrease the NO trapping probability of the monolayer film compared to the multilayer films. The S_0 on the multilayer ttbu-FePc film may be attributed to fewer metal, aromatic, and nitrogen sites being exposed to the incoming beam due to its lower packing density. Since NO chemisorption occurs on 100% of the surface Fe metal center sites for all three films, the saturation coverage is less on the multilayer ttbu-FePc film than on the ordered monolayer and multilayer FePc films as a result of the area occupied by the Fe metal being less in the lower areal density ttbu-FePc film than in the monolayer and multilayer FePc films.

ACKNOWLEDGMENTS

Funding was provided by AFOSR MURI F49620-02-1-0288 and NSF CHE-0350571. The SRC AMD Graduate Fellowship provided funding for S.R.B. The Department of Homeland Security appointed Ngoc L. Tran to the U.S. Department of Homeland Security (DHS) Scholarship and Fellowship Program, administered by the Oak Ridge Institute for Science and Education (ORISE) through an interagency agreement between the U.S. Department of Energy (DOE) and DHS. ORISE is managed by Oak Ridge Associated Universities (ORAU) under DOE Contract No. DE-AC05-06OR23100. All opinions expressed in this paper are the author's and do not necessarily reflect the policies and views of DHS, DOE, or ORAU/ORISE.

[1] R. P. Linstead and F. T. Weiss, J. Chem. Soc. **11**, 2981 (1950).
[2] N. H. Sabelli and C. A. Melendres, J. Phys. Chem. **86**, 4342 (1982).
[3] M. V. Zeller and R. G. Hayes, J. Am. Chem. Soc. **95**, 3855 (1973).
[4] B. Bott and T. Jones, Sens. Actuators B **5**, 43 (1984).
[5] J. D. Wright, Prog. Surf. Sci. **31**, 1 (1989).
[6] R. Gould, Coord. Chem. Rev. **156**, 237 (1996).
[7] J. Germain, A. Pauly, C. Maleysson, J. Blanc, and B. Schollhorn, Thin Solid Films **333**, 235 (1998).
[8] B. Schollhorn, J. Germain, A. Pauly, C. Maleysson, and J. Blanc, Thin Solid Films **326**, 245 (1998).
[9] J. C. Buchholz, Appl. Surf. Sci. **1**, 547 (1978).
[10] R. L. Vanewyk, A. V. Chadwick, and J. D. Wright, J. Chem. Soc., Faraday Trans. 1 **76**, 2194 (1980).
[11] R. L. Vanewyk, A. V. Chadwick, and J. D. Wright, J. Chem. Soc., Faraday Trans. 1 **77**, 73 (1981).
[12] F. I. Bohrer, C. N. Colesniuc, J. Park, I. K. Schuller, A. C. Kummel, and W. C. Trogler, J. Am. Chem. Soc. **130**, 3712 (2008).
[13] F. I. Bohrer, A. Sharoni, C. Colesniuc, J. Park, I. K. Schuller, A. C. Kummel, and W. C. Trogler, J. Am. Chem. Soc. **129**, 5640 (2007).
[14] R. D. Yang, J. E. Park, C. N. Colesniuc, I. K. Schuller, W. C. Trogler, and A. C. Kummel, J. Chem. Phys. **130**, 164703 (2009).
[15] M. Bora, D. Schut, and M. A. Baldo, Anal. Chem. **79**, 3298 (2007).
[16] J. Brunet, A. Pauly, L. Mazet, J. P. Germain, M. Bouvet, and B. Malezieux, Thin Solid Films **490**, 28 (2005).
[17] S. Bishop, N. Tran, G. Poon, and A. Kummel, J. Chem. Phys. **127**, 214702 (2007).
[18] N. Tran and A. Kummel, J. Chem. Phys. **127**, 214701 (2007).
[19] K. Miller, R. Yang, M. Hale, J. Park, B. Fruhberger, C. Colesniuc, I. Schuller, A. Kummel, and W. Trogler, J. Phys. Chem. B **110**, 361 (2006).
[20] R. D. Yang, B. Fruhberger, J. Park, and A. C. Kummel, Appl. Phys. Lett. **88**, 074104 (2006).
[21] T. F. Hanisco and A. C. Kummel, J. Phys. Chem. **95**, 8565 (1991).
[22] K. A. Pettus, T. S. Ahmadi, E. J. Lanzendorf, and A. C. Kummel, J. Chem. Phys. **110**, 4641 (1999).
[23] G. C. Poon, T. J. Grassman, J. C. Gumy, and A. C. Kummel, J. Chem. Phys. **119**, 9818 (2003).
[24] J. V. Barth, H. Brune, G. Ertl, and R. J. Behm, Phys. Rev. B **42**, 9307 (1990).
[25] M. Ondrejcek, M. Rajappan, W. Swiech, and C. P. Flynn, Surf. Sci. **574**, 111 (2005).
[26] D. A. King and M. G. Wells, Surf. Sci. **29**, 454 (1972).
[27] D. A. King and M. G. Wells, Proc. R. Soc. London, Ser. A **339**, 245 (1974).
[28] S. F. Alvarado, L. Rossi, P. Muller, and W. Riess, Synth. Met. **122**, 73 (2001).
[29] K. Manandhar, T. Ellis, K. T. Park, T. Cai, Z. Song, and J. Hrbek, Surf. Sci. **601**, 3623 (2007).
[30] I. Chizhov, G. Scoles, and A. Kahn, Langmuir **16**, 4358 (2000).
[31] W. Eberhardt and M. Hanack, Synthesis **1**, 95 (1997).
[32] B. Gorlach, M. Dachtler, T. Glaser, K. Albert, and M. Hanack, Chem.-Eur. J. **7**, 2459 (2001).
[33] I. Biswas, H. Peisert, L. Zhang, T. Chasse, M. Knupfer, M. Hanack, D. Dini, T. Schmidt, and D. Batchelor, Mol. Cryst. Liq. Cryst. **455**, 241 (2006).
[34] A. M. Wodtke, H. Yuhui, and D. J. Auerbach, Chem. Phys. Lett. **413**, 326 (2005).
[35] C. R. Arumainayagam and R. J. Madix, Prog. Surf. Sci. **38**, 1 (1991).
[36] A. T. Gee, B. E. Hayden, C. Mormiche, A. W. Kleyn, and B. Riedmuller, J. Chem. Phys. **118**, 3334 (2003).
[37] L. Vattuone, L. Savio, M. Okada, K. Moritani, and M. Rocca, Surf. Sci. **602**, 2689 (2008).
[38] M. P. Develyn, H. P. Steinruck, and R. J. Madix, Surf. Sci. **180**, 47 (1987).
[39] D. C. Seets, M. C. Wheeler, and C. B. Mullins, Chem. Phys. Lett. **257**, 280 (1996).
[40] M. Takada and H. Tada, Chem. Phys. Lett. **392**, 265 (2004).
[41] R. D. Yang, T. Gredig, C. Colesniuc, J. E. Park, I. Schuller, W. Trogler, and A. C. Kummel, Appl. Phys. Lett. **90**, 263506 (2007).
[42] A. J. Komrowski, K. Ternow, B. Razaznejad, B. Berenbak, J. Z. Sexton, I. Zoric, B. Kasemo, B. I. Lundqvist, S. Stolte, A. W. Kleyn, and A. C. Kummel, J. Chem. Phys. **117**, 8185 (2002).
[43] Referee, personal communication (October 2, 2008).